Applied Acoustics 183 (2021) 108331

Contents lists available at ScienceDirect

Applied Acoustics

journal homepage: www.elsevier.com/locate/apacoust

Study of probe signal bandwidth influence on estimation of coherence bandwidth for underwater acoustic communication channel

Iwona Kochanska [a,1,*], Jan H. Schmidt [a,2], Aleksander M. Schmidt [a,3]

[a] Gdansk University of Technology, Faculty of Electronics, Telecommunications and Informatics, G. Narutowicza 11/12, 80-233 Gdansk, Poland

ARTICLE INFO

Article history:
Received 10 February 2021
Received in revised form 2 July 2021
Accepted 26 July 2021
Available online 10 August 2021

Keywords:
underwater acoustic communications
impulse response measurement
coherence bandwidth

ABSTRACT

A signal transmitted in a shallow Underwater Acoustic Communication (UAC) channel suffers from time dispersion due to the multipath propagation and the refraction phenomena. This causes intersymbol interference of the received signal and frequency-selective fading observed in its spectrum. Coherence bandwidth is one of the key transmission parameters used for designing the physical layer of a data transmission system to minimise the influence of time dispersion on the received signal. It can be calculated on the basis of the channel impulse response, measured with the use of the correlation method and frequency modulated signals or pseudorandom binary sequences. Such signals have a narrow, impulse-like autocorrelation function if considered in baseband. However, in the case of bandpass measurements, the influence of the probe signal on the estimate of the impulse response, and thus on the estimate of transmission parameters, is no longer negligible. The paper presents the results of an experimental study on probe signal bandwidth influence on estimation of coherence bandwidth. Simulations were carried out using UAC channel impulse responses measured in an inland reservoir.

1. Introduction

The bit rate achieved in UAC systems is much lower than for wire or radio-communication systems. This is due to the disadvantageous properties of the UAC channels, namely the sea and inland waters, but is also due to the technical capabilities of the generation and reception of acoustic waves. Within a limited bandwidth, the signal is subject to multipath propagation through a channel whose characteristics vary with time and are highly dependent on the location of the transmitter and receiver. While vertical channels exhibit little time-dispersion, horizontal channels may have extremely large multipath spreads. In a digital communication system multipath propagation causes Inter-Symbol Interference (ISI), which can be expressed as the multipath spread in terms of symbol intervals. In the case of medium-range shallow water UAC system multipath propagation may cause the ISI to extend over 100 transmitted symbols [8]. The multipath propagation phenomenon goes hand-in–hand with strong refraction, caused by a significant change in sound velocity as a function of depth [5]. Both multipath propagation and refraction produce time dispersion of the transmitted signal, the consequence of which is frequency-selective fading observed in the frequency response of the channel. This has a degrading influence on the ability to correctly detect transmitted information. Minimizing this impact requires adaptation of the modulation and coding scheme to the propagation conditions in the communication channel.

Coherence bandwidth B_c is a statistical measure of the range of frequencies over which the channel is not affected with frequency-selective fading. It is a maximal frequency range, wherein the amplitude characteristic of the channel remains constant and its phase characteristic is linear [19,7]. In the case of single-carrier system, the signal bandwidth is selected to be smaller than B_c to avoid frequency-selective fading [19,18]. In the case of multi-carrier system, the coherence bandwidth determines the maximal subcarrier spacing [19,11,9,13].

The coherence bandwidth is calculated on the basis of the Time-Varying Impulse Response (TVIR) of the underwater acoustic channel. The direct measurement of such a TVIR requires exciting the tested channel with short pulses having flat spectrum in the whole frequency band of the system transfer function. However, the pulses generated by acoustic measurement equipment have energy sufficient mere in laboratory conditions – in small rooms and test tanks [12]. It is difficult to generate a signal that imitates a Dirac pulse well, with a very high concentration of energy over

* Corresponding author.
E-mail addresses: iwona.kochanska@pg.edu.pl (I. Kochanska), jan.schmidt@pg.edu.pl (J.H. Schmidt), aleksander.schmidt@pg.edu.pl (A.M. Schmidt).
[1] ORCID: 0000-0001-8401-3930
[2] ORCID: 0000-0002-2051-9147
[3] ORCID: 0000-0003-2538-5173

https://doi.org/10.1016/j.apacoust.2021.108331
0003-682X/

time. In underwater acoustic measurements, the source of such an impulse may be an explosive. There are explosive sound sources, like SUS (Signal, Underwater Sound), used for generating high amplitude pulses directly in the propagation medium [2,3]. However, the influence of underwater explosion does not constitute a single impulse but a few large energy pulsations of gas bubbles [6]. Moreover, pulse signals generated with an explosive sound source is difficult to synchronize – first, when repetition is needed, and second, for synchronized reception.

For this reason, the TVIR of UAC channel is commonly measured by correlation method [1]. In this method, probe signals having a wide frequency spectrum are used, namely Pseudo-Random Binary Sequence (PRBS) and Linear Frequency-Modulated (LFM) chirp trains [22]. The PRSB signal is constructed of the pseudo-noise sequence, which is upsampled to achieve a desired binary switching rate, commonly referred to as the 'chipping' rate, which, in turn, determines the bandwidth of the probe signal. Such an upsampled binary sequence is used to modulate the carrier frequency according to the Binary Phase Shift Keying (BPSK) technique [22,20,21,17]. The LFM chirp train signal is a sinusoid with lineary increasing frequency from minimal to maximal value. The difference between these values determines the bandwidth in which the measurement is performed. Also the Hyperbolic Frequency-Modulated chirps (HFM) can be used for the UAC channel sounding. Such a signal is a sinusoid with exponentially increasing frequency [17]. At the receiver site, the measured PRBS signals, as well as LFM and HFM chirps, are passed through the filter matched to a single transmitted probe signal. The signal at the output of the matched filter represents the TVIR of the channel.

In this paper the PRBS probe signal is considered. It has a narrow, impulse-like autocorrelation function if considered in baseband. Such an autocorrelation function allows the influence of the probe signal on the impulse response estimate to be minimised. However, in the case of bandpass PRBS measurement, the deterioration of the correlation property of bandlimited probe signals is observed, and the influence of its autocorrelation function on the estimate of impulse response is no longer negligible. This may lead to incorrect estimation of the coherence bandwidth and, as a consequence, to setting such parameters of the physical layer of data transmission that will not ensure the best possible rate or reliability of communication.

Although bandlimited PRBS signals are often used for UAC channel sounding, to the best of the authors' knowledge, there are no publications on the impact of the probe signal bandwidth on the estimate of the coherence bandwidth. This problem does not arise in the case of shallow channels, in which there are conditions of strong multipath propagation. In such cases the coherence bandwidth is often of the order of single or tens of hertz, and the probe signal has a bandwidth that is many times greater, of the order of kHz [22]. However, in vertical channel or in horizontal deep ocean channel, where there is a little time-dispersion of the received signal, the coherence bandwidth of the channel may be of the same order as the bandwidth of the probe signal, and the influence of the latter one on the estimate of this transmission parameter may not be negligible.

The problem of the estimation of coherence bandwidth of the UAC channel was previously mentioned in the conference paper [10]. In this paper we present a more detailed analysis of this problem, which is extended with the results of simulation tests obtained using replay UAC channel model based on the impulse responses measured in an inland reservoir. The goal of the tests performed was to assess the influence of the probe signal bandwidth on the estimated coherence bandwidth and to determine what the signal bandwidth should be in relation to the B_c parameter so that its influence on B_c estimation is negligible. The knowledge acquired during these tests can be used to achieve greater accuracy in the estimation of the coherence bandwidth, which is used for designing the modulation and coding schemes of modern UAC systems, i. e. Orthogonal Frequency-Division Multiplexing (OFDM) systems and spread spectrum systems with frequency hopping technique [9,16].

2. Bandlimited probe signal for UAC impulse response measurement

The channel impulse response measurement is usually performed by the correlation method using the probe signal, which has a narrow, impulse-like autocorrelation function if considered in baseband. A Pseudo-Random Binary Sequence (PRBS) is one type of signals that meets this requirement [22,20]. The Power Spectral Density (PSD) of the baseband PRBS is constant for all the discrete frequencies in the covered frequency band, except for the DC offset. Such truly wideband sequences are used for measurements, inter alia, in room acoustics or building acoustics [15,4].

In underwater acoustics, bandpass PRBS signals of limited bandwidth are used. The pseudo-random sequence is upsampled by a factor of R and passed through a Zero-Order Hold (ZOH) filter of transfer function given by [14]:

$$H_{ZOH}(f) = T\frac{sin(\pi fT)}{\pi fT}e^{-j\pi fT},\ T = R/f_s \tag{1}$$

where f_s is the sampling rate. Next, a complex-value representation of the PRBS is obtained with the use of a Hilbert transform. Such a baseband probe signal $s(t)$ is used to modulate the carrier waveform of frequency f_c.

At the receiver side a recorded signal is brought to the complex baseband and downsampled. Next, the matched filtration is performed. As a result an estimate $\hat{h}(t)$ of impulse response is obtained, which is a convolution of the channel impulse response $h(t)$ and the autocorrelation function of probe signal $R_s(\Delta t) = E[s(t)s^*(t+\Delta t)]$. Thus, in the frequency domain, the estimate of channel transfer function $\widehat{H}(f)$ is equal to:

$$\hat{H}(f) = H(f)H_s(f) \tag{2}$$

where the transfer functions: $\hat{H}(f), H(f)$, and the power spectral density $H_s(f)$ are calculated as the Fourier transforms of $\hat{h}(t), h(t)$, and $R_s(\Delta t)$, respectively.

3. Estimation of coherence bandwidth

The coherence bandwidth B_c is obtained on the basis of the Space-Frequency Correlation Function (SFCF) $R_H(\Delta f)$, which is calculated as the autocorrelation of the channel transfer function $H(f)$:

$$R_H(\Delta f) = E[H(f)H^*(f+\Delta f)] \tag{3}$$

The coherence bandwidth B_c is calculated as the width of $R_H(\Delta f)$ at a given threshold T_R. Usually T_R is equal to 0.5 of the maximum value of $R_H(\Delta f)$ [19].

In case of channel measurement performed by correlation method, SFCF is affected by the influence of the bandlimited probe signal. Fig. 1 shows the results of simulation test performed in Matlab environment. A probe signal was convolved with the impulse response $h(t)$ measured during the inland water experiment. The PRBS probe signal of bandwidth $B_s = 2\ kHz$ was constructed of an m-sequence of rank $L = 10$. As a result of the simulation test the estimate of theimpulse response $\hat{h}(t)$ was obtained, which corresponds to the bandlimited transfer function $\hat{H}(f)$. The Space-Frequency Correlation Function $R_{\hat{H}}(\Delta f) = E\left[\hat{H}(f)\hat{H}^*(f+\Delta f)\right]$ was

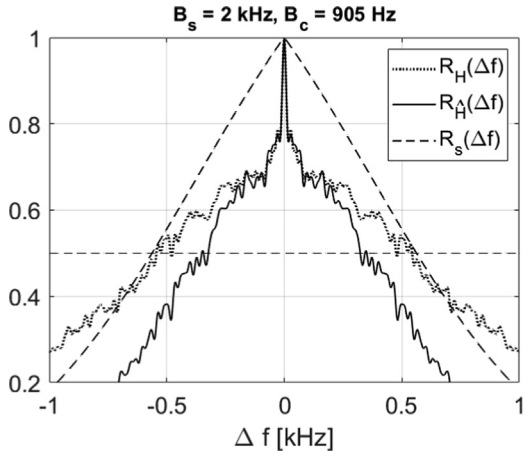

Fig. 1. The influence of the probe signal autocorrelation function in frequency domain ($R_s(\Delta f)$) on estimated SFCF of the channel ($R_{\hat{H}}(\Delta f)$); $R_H(\Delta f)$ – real SFCF of the channel; B_s – probe signal bandwidth; B_c- coherence bandwidth of the channel.

calculated on the basis of the transfer function $\hat{H}(f)$, and the $R_H(\Delta f)$ is given by Eq. (3). The characteristic $R_s(\Delta f) = E[H_s(f)H_s^*(f+\Delta f)]$ corresponds to the autocorrelation function of the probe signal PSD. It is clearly seen that $R_H(\Delta f)$ and $R_{\hat{H}}(\Delta f)$ have different shapes, which results in different values of the coherence band B_c measured at the threshold level $T_R = 0.5$.

The relationship of the Space-Frequency Correlation Function $R_H(\Delta f)$ and $R_{\hat{H}}(\Delta f)$ can be described as:

$$R_{\hat{H}}(\Delta f) = E[H(f)H^*(f+\Delta f)H_s(f)H_s^*(f+\Delta f)] = R_H(\Delta f)R_s(\Delta f) + C(\Delta f) \tag{4}$$

where:

$$C(\Delta f) = cov(H(f)H^*(f+\Delta f), H_s(f)H_s^*(f+\Delta f)) \tag{5}$$

according to a relationship of expected values of a product of two stochastic processes: $E[XY] = E[X]E[Y] + cov(X,Y)$. Eq. (4) can be simplified to $R_{\hat{H}}(\Delta f) = R_H(\Delta f)R_s(\Delta f)$, when $H(f)$ and $H_s(f)$ represent independent processes.

A time-domain autocorrelation function of impulse response of ZOH filter $R_s(\Delta t)$ is a triangular function, which can be described as:

$$R_s(\Delta t) = \begin{cases} 1 + \frac{\Delta t}{T} & \text{if } -T \leqslant \Delta t < 0 \\ 1 - \frac{\Delta t}{T} & \text{if } 0 \leqslant \Delta t < T \end{cases} \tag{6}$$

Its PSD $H_s(f)$ calculated as the Fourier transform of $R_s(\Delta t)$ is the same as $H_{ZOH}(f)$ described by Eq. (1). The autocorrelation function in frequency domain $R_s(\Delta f)$ is equal to:

$$\begin{aligned} R_s(\Delta f) &= E[H_s(f)H_s^*(f+\Delta f)] \\ &= T^2\left(\frac{1}{\pi^2\Delta f^2 T} - \frac{\sin(2\pi\Delta f T)}{2\pi^3\Delta f^3 T^2}\right) \end{aligned} \tag{7}$$

To minimize the influence of the probe signal on the estimated $R_{\hat{H}}(\Delta f)$ and thus on the coherence bandwidth B_c, values of $R_s(\Delta f)$ should be close to 1 in the bandwidth equal to the estimated coherence bandwidth. If B_c is measured at 0.5 of $R_{\hat{H}}(\Delta f)$, it must be ensured that $R_s(\Delta f)$ has values close to 1 in this range.

4. Simulation tests

The influence of bandlimitation of the probe signal on the coherence bandwidth B_c value was tested using the UAC replay channel, simulated by channel impulse responses measured in Wdzydze Lake in Poland. During the inland water experiment the transmission side was placed on the boat and the transmission transducer was sunk to a depth of 10 metres, where the depth of water was about 20 metres. The receiving equipment was placed in a measuring container, and the receiving transducer was sunk to a depth of 4 m, where the depth of water was about 7 m. The distance between the transmitter and receiver positions was 330, 550 or 1035 m. Measurements were carried out on two consecutive days: May 4 and 5, 2017. On the first day, when an experiment was performed at a distance of 550 m, the weather was windy and it was raining. The next day, during the measurements at distances of 330 m and 1035 m, the weather was windless; it was not raining and the water surface was calm. Channel Time-Varying Impulse Response (TVIR) was measured by the correlation method with the use of PRBS signal, based on an m-sequence of rank 8 and 10. The carrier frequency f_c and the sampling rate f_s in each case

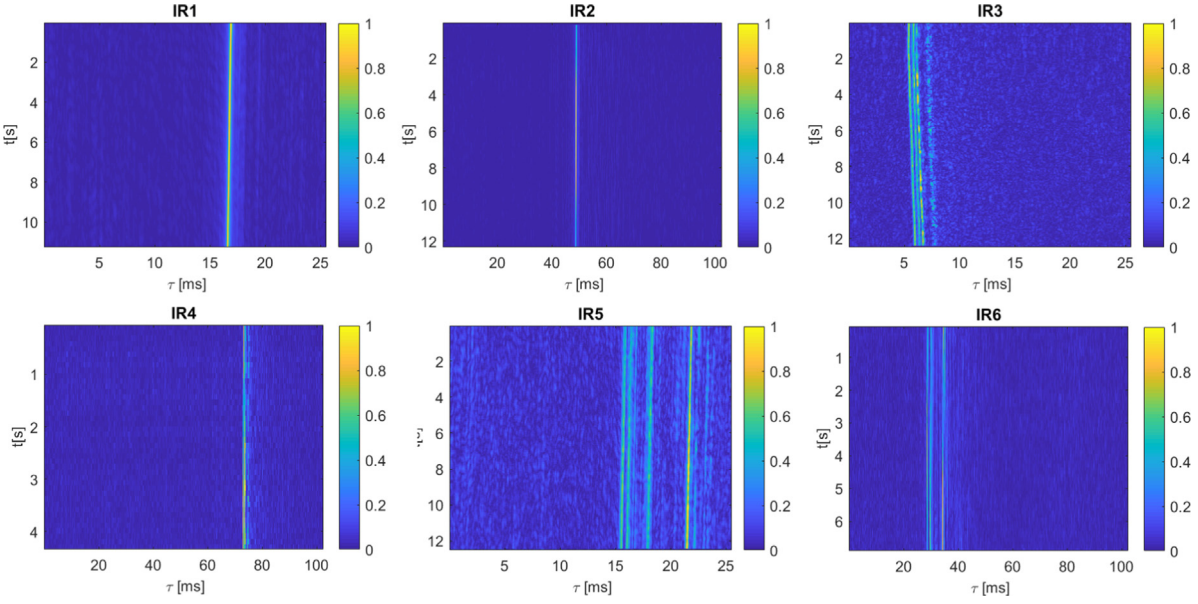

Fig. 2. Modules of TVIRs of underwater channel measured during the inland water experiment.

was equal to 30 kHz and 200 kHz, respectively. The bandwidth B of the probe signal was equal to 10 kHz.

In the case of a bandlimited bandpass channel, channel impulse reponse is equivalently described by a complex baseband Time-Varying Impulse Response $h(t,\tau)$, defined in a window of observation time t and delay τ. In *tau* domain the resolution of $h(t,\tau)$ is equal to $1/f_s$. A maximum value of delay τ is a duration of a single realisation of TVIR. It is equal to a single probe sequence duration, that is $T_s = \frac{R \cdot L}{f_s}$, where L denotes number of m-sequence bits and R denotes upsampling factor, which was equal to $\frac{f_s}{B} = 20$ during the experiment. In case of m-sequence of rank 8, T_s was equal to $\frac{20 \cdot 255}{200\ \text{kHz}} = 25.5$ ms, and in case of m-sequence of rank 10 it is was equal to $\frac{20 \cdot 1023}{200\ \text{kHz}} = 102.3$ ms. The probe sequence was repeated numerous times, which allowed to get up to 480 realisations of impulse response using m-sequence of rank 8, and up to 120 realisation of $h(t,\tau)$ using m-sequence of rank 10. The modules of six TVIRs gathered during the experiment are shown in Fig. 2. For each of TVIRs, the Space-Frequency Correlation Function was calculated. The resolution of SFCF in frequency domain is equal to $\frac{1}{T_s}$, that is 39.22 Hz in case of SFCF calculated on the basis of TVIR measured with the use of m-sequence of rank 8, and 9.78 Hz in case of SFCF calculated on the basis of TVIR measured with the use of m-sequence of rank 10. The coherence bandwidth was obtained as the width of SFCF at a threshold level of 0.5 of its maximum value. The coherence bandwidth values are shown in Table 1.

Fig. 3 shows the SFCFs $R_H(\Delta f)$ corresponding to three of measured TVIRs, and the probe signal PSD autocorrelation function $R_s(\Delta f)$. It is clearly seen, that the influence of probe signal of bandwidth $B = 10\ kHz$ on the coherence bandwidth B_c estimate is negligible due to values of normalized $R_s(\Delta f)$ close to 1 for $\Delta f = f_1$ and $\Delta f = f_2$, where f_1 and f_2 are the values for which normalized $R_H(\Delta f)$ is equal to 0.5 (and thus the coherence bandwidth is equal to $B_c = f_2 - f_1$).

The simulation tests were performed in Matlab environment. From each TVIR, 22 realizations of impulse response $h(t_n,\tau), n = 0,1,\ldots,(N-1), N = 22$, were selected to simulate stationary UAC channels with multipath propagation. Probe signal $s(t)$ of a different bandwidth, varying from 100 Hz to 8 kHz, was transmitted through such channels, to check what is the influence of $s(t)$ on the coherence bandwidth estimate.

During the simulation tests the received signal $y(t)$ was calculated as the convolution of the probe signal $s(t)$ and a single realisation of the impulse response $h(t_n,\tau)$. At the simulated receiver side, matched filtration was performed, and new impulse response estimates $\hat{h}(t,\tau)$ were obtained. For each impulse response estimate the corresponding transfer function $\hat{H}(f)$ and frequency correlation function $R_{\hat{H}}(\Delta f)$were calculated. Finally, the coherence bandwidth $\hat{B}_c$ was obtained as the width of $R_{\hat{H}}(\Delta f)$at the threshold level $T_R = 0.5$ of its maximum value.

Table 1
Parameters of TVIRs of underwater channel, measured during the inland water experiment.

IR number	Distance	m-sequence rank	coherence bandwidth
IR1	330 m	8	2745.1 Hz
IR2	330 m	10	2834.8 Hz
IR3	550 m	8	549.0 Hz
IR4	550 m	10	469.2 Hz
IR5	1035 m	8	156.9 Hz
IR6	1035 m	10	117.3 Hz

5. Results

The values of the coherence bandwidth estimate $\hat{B}_c$, averaged over 22 simulation tests performed for each of 6 TVIRs measured during the inland water experiment, are shown in Fig. 4. The dashed line indicates the coherence bandwidth B_c values calculated on the basis of measured TVIR, and the blue marks present the values of the coherence bandwidth $\tilde{B}_c$ calculated as the width of $\tilde{R}_H(\Delta f)$ defined as:

$$\tilde{R}_H(\Delta f) = R_H(\Delta f) R_s(\Delta f) \tag{8}$$

$\tilde{R}_H(\Delta f)$ is a SFCF which would be achieved if the transfer function $H(f)$ of the UAC channel and the probe signal PSD $H_s(f)$ were mutualy independent. $\tilde{B}_c$ is calculated at the threshold level equal to 0.5 of the maximum value of $\tilde{R}_H(\Delta f)$.

Additionally, Fig. 4 shows the values of the root mean squared error E_B calculated according to the following equation:

$$E_B = \sqrt{\frac{1}{N}\sum_{i=1}^{N}\left(\hat{B}_c - B_c\right)^2} \tag{9}$$

where $N = 22$ is the number of tests performed for each probe signal bandwidth value B_s, with the use of a set of realisations of a given TVIR. Fig. 5 presents all the root mean squared error E_B values presented in Fig. 4, relative to the coherence bandwidth B_c value, as a function of the probe signal bandwidth B_s relative to B_c.

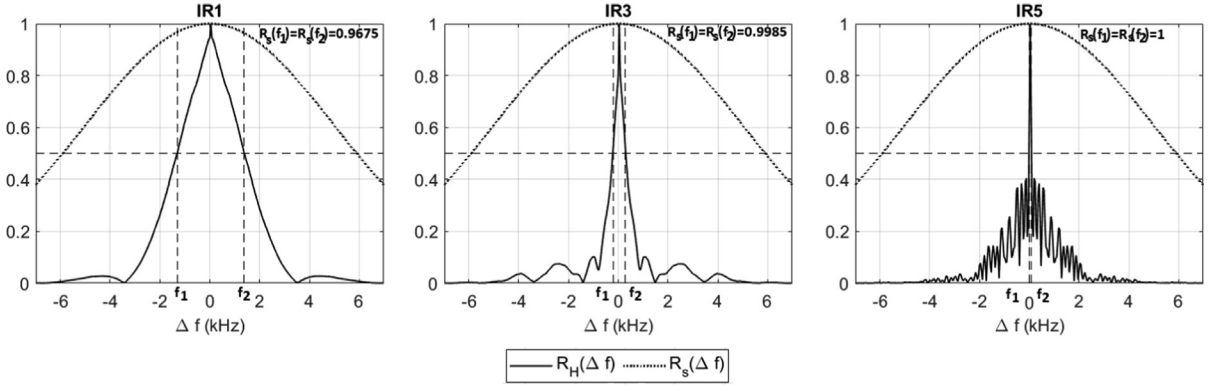

Fig. 3. Normalized probe signal PSD autocorrelation function ($R_s(\Delta f)$) and normalized SFCFs ($R_H(\Delta f)$) of the UAC channels measured during the inland water experiment; $B_c = f_2 - f_1$.

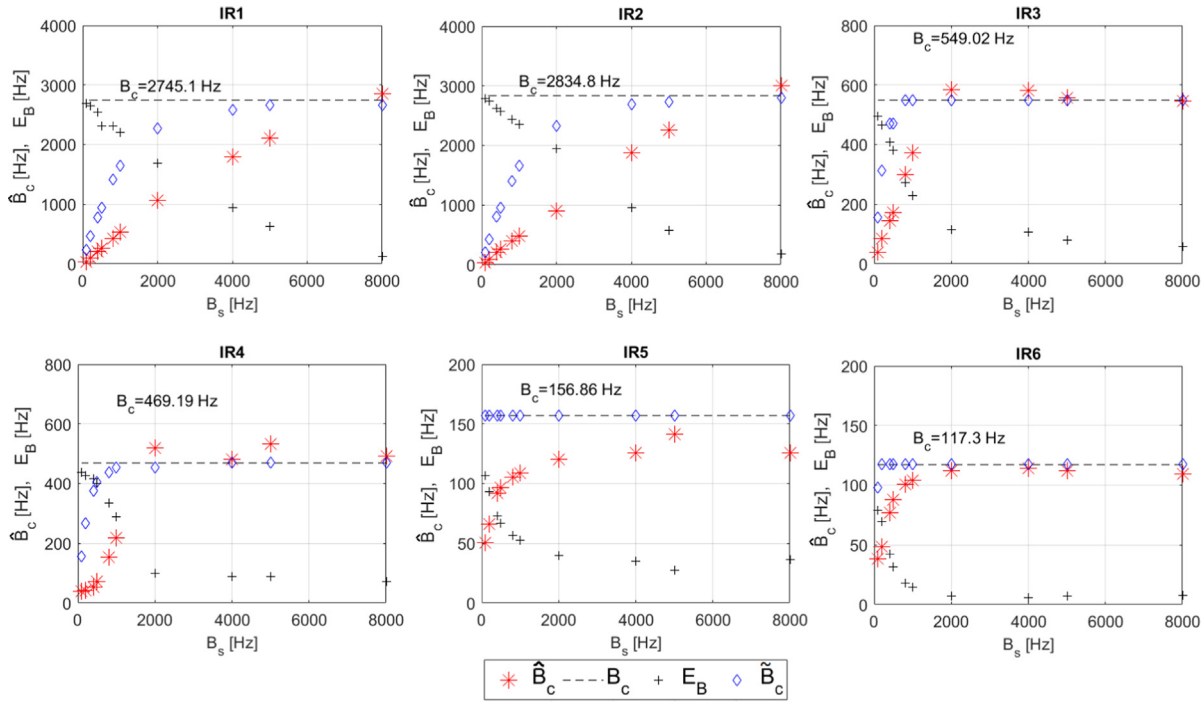

Fig. 4. $\hat{B}_c$ estimate values averaged over 20 simulation tests (*), the rms error E_B (+), and $\tilde{B}_c$ (◆) calculated under assumption, that the chanel transfer function $H(F)$ and probe signal PSD $H_s(f)$ are mutually independent.

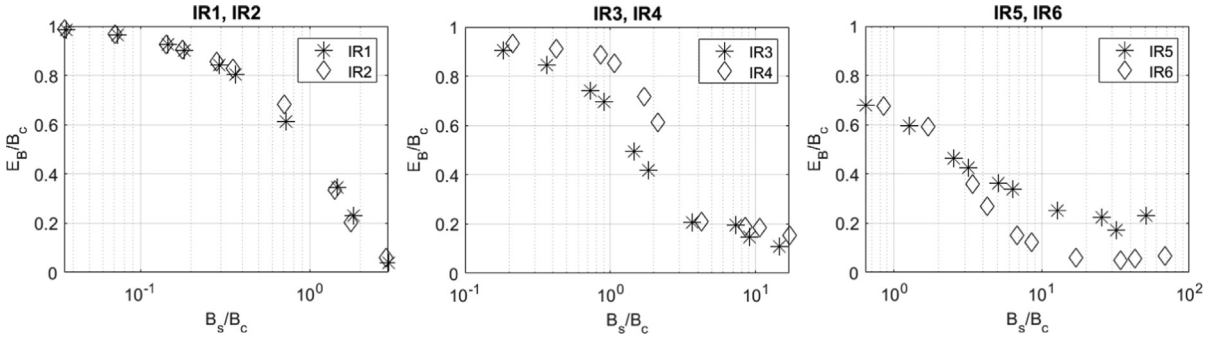

Fig. 5. The root mean squared error E_b values for all simulation tests with the use of impulse response IR1-IR6, relative to the coherence bandwidth B_c as a function of the probe signal bandwidth B_s relative to B_c.

6. Discussion

As it can be seen in Fig. 4, for IR1 and IR2, corresponding to the UAC channel at a distance of 330 m, the values of $\hat{B}_c$are close to the measured coherence banwidth B_c, which is equal to 2745.1 Hz and 2834.8 Hz, respectively, when the probe signal has a bandwidth B equal to 8 kHz. Thus, for B almost 3 times larger than B_c the root mean squared error of $\hat{B}_c$ is less than 0.06 B_c (Fig. 5).

In case of IR3 and IR4 impulse responses, for which the coherence bandwidth B_c is equal to 549.02 Hz and 469.19 Hz, respectively, the estimates $\hat{B}_c$ are close to B_c when the measurement signal has a bandwidth of at least $B = 2$ kHz. Such a probe signal provides the root mean squared error of about 0.2 B_c. The smallest E_B was obtained using the probe signal of bandwidth equal to 8 kHz. It was equal to 0.15 B_c in case of the IR3 response and 0.1 B_c in case of the IR4 response. It is worth noting that the IR3 and IR4 impulse responses were measured during bad weather conditions and strongly waving water surface, which could have influenced the relatively high $E_B$obtained during the simulation with the use of these TVIRs.

In case of IR5, none of the probe signals allowed to obtain an estimate of $\hat{B}_c$ close to B_c equal to 156.86 Hz. This is probably due to the fact that the SFCF frequency resolution for IR5, and thus the smallest possible error of the coherence bandwidth estimation, is equal to 39.22 Hz, which is as much as 25% of the B_c value. In case of other responses measured by the probe signal based on m-sequence of rank 8, the frequency resolution does not have such a significant effect on the estimation error, because for IR1 the resolution equal to 39.22 Hz is 1.43% of B_c and for IR3 it is 7.14% of B_c.

In case of IR6, a probe signal of bandwidth equal to at least 2 kHz allowed to obtain $\hat{B}_c$ with estimation error less than 0.05B_c.

The results obtained indicate that the estimation of the coherence bandwidth of the UAC channel on the basis of the impulse response, measured by correlation method, is possible with limited accuracy. In order to ensure the highest possible accuracy, the impulse response of the channel could be measured using a probe signal with a gradually increased bandwidth to the value achievable in the measurement system. It could be checked online if the coherence estimate changes significantly when the probe signal bandwidth increases. No significant differences between the

successive $\hat{B}_c$ estimates would then indicate that the highest possible accuracy has been achieved. Such an approach increases the time and the number of calculations needed to determine the coherence bandwidth in proportion to the number of measurements performed. However, this does not increase the computational complexity of the $B_c$parameter determination procedure, which depends on the computational complexity of the algorithms of matched filtering and calculation of transfer function and its autocorrelation function. Additionally, during the coherence bandwidth estimation, it should be checked, if the ratio of the B_c estimate and the probe signal bandwidth B_s is such that the value of PSD autocorrelation function $R_s(0.5B_c)$ is close to 1.

CRediT authorship contribution statement

Iwona Kochanska: Methodology, Software, Formal analysis, Writing - original draft. **Jan H. Schmidt:** Conceptualization, Validation, Investigation, Resources, Writing - review & editing. **Aleksander M. Schmidt:** Validation, Investigation, Data curation, Visualization.

Declaration of Competing Interest

The authors declare that they have no known competing financial interests or personal relationships that could have appeared to influence the work reported in this paper.

References

[1] Bjorno L. Underwater acoustic measurements and their applications. Applied Underwater Acoustics. Elsevier; 2017. p. 889–947.
[2] Chapman NR. Source levels of shallow explosive charges. The Journal of the Acoustical Society of America 1988;84(697). https://doi.org/10.1121/1.396849.
[3] Dicus RL. Impulse response estimation with underwater explosive charge acoustic signals. The Journal of the Acoustical Society of America 1981;70 (122). https://doi.org/10.1121/1.386690.
[4] Dobrucki A, Brachmański S. Test signals used in electroacoustics and speech technology. In: 2017 Signal Processing: Algorithms, Architectures, Arrangements, and Applications. IEEE; 2017. p. 15.
[5] Grelowska G., Kozaczka E., Witos-Okrasińska D., Vertical temperature stratification of the gulf of gdansk water. In: Proceedings of 2018 Joint Conference – Acoustics; 2018: 80–85.
[6] Grzadziela A. Model of impact underwater detonation. Journal of KONES Powertrain and Transport 2012;19:191–9.
[7] Hlawatsch F, Matz G. Wireless communications over rapidly time-varying channels. Academic Press; 2011.
[8] Istepanian R, Stojanovic M. Underwater acoustic digital signal processing and communication systems. Springer Sciences+Business Media; 2002.
[9] Kochanska I. Reliable ofdm data transmission with pilot tones and error-correction coding in shallow underwater acoustic channel. Applied Sciences 2020;10:2173.
[10] Kochanska I., Schmidt J. H., Estimation of coherence bandwidth for underwater acoustic communication channel. In: Proceedings of 2018 Joint Conference – Acoustics. 2018:130-133.
[11] Kochanska I, Schmidt J, Marszal J. Shallow water experiment of OFDM underwater acoustic communications. Archives of Acoustics 2020;45(1):11–8.
[12] Mazurek R, Lasota H. Application of maximum-length sequences to impulse response measurement of hydroacoustic communications systems. Hydroacoustics 2007;10:123–30.
[13] Nissen I. Pilot-based ofdm-systems for underwater communication applications. In: Proceedings conference on new concepts for harbour protection, littoral security and underwater acoustic communications (TICA).
[14] Oppenheim AV. Signals and systems. Prentice-Hall Signal Processing Series. 1982.
[15] Riffe DD, Vanderkooy J. Transfer-function measurement with maximum-length sequences. Journal of the Audio Engineering Society 1989;37:419–43.
[16] Schmidt JH. Using fast frequency hopping technique to improve reliability of underwater communication system. Applied Sciences 2020;10(3):1172.
[17] Schmidt JH, Kochansa I, Schmidt AM. Measurement of impulse response of shallow water communication channel by correlation method. Hydroacoustics 2017;20:149–58.
[18] Schmidt J. H., Schmidt A. M., Kochanska I., Multiple-input multiple-output technique for underwater acoustic communication system. In: Proceedings of 2018 Joint Conference – Acoustics; 2018: 280–283.
[19] Sklar B. Rayleigh fading channels in mobile digital communication systems. I. Characterization. IEEE Communications Magazine 1997;35:90–100.
[20] Studanski R, Zak A. Measurement of hydroacoustic channel impulse response. Applied Mechanics and Materials 2016;817:317–24.
[21] Studanski R, Zak A. Results of impulse response measurements in real conditions. Journal of Marine Engineering & Technology 2017;16(4):337–43.
[22] van Walree P. Channel sounding for acoustic communications: techniques and shallow-water examples; FFI-Rapport 2011/00007. Forsvarets 2011. forskningsinstitutt.